Sensors & Actuators: B. Chemical 350 (2022) 130858

Contents lists available at ScienceDirect

Sensors and Actuators: B. Chemical

journal homepage: www.elsevier.com/locate/snb

# Polymeric microsphere enhanced surface plasmon resonance imaging immunosensor for occult blood monitoring

Jie Zhou [a], Xueliang Wang [a], Jiajie Chen [a,*], Youjun Zeng [a], Dayong Gu [b], Bruce Zhi Gao [c], Yonghong Shao [a,*]

[a] College of Physics and Optoelectronic Engineering, Key Laboratory of Optoelectronic Devices and Systems of Ministry of Education and Guangdong Province, Shenzhen University, Shenzhen 518060, China
[b] Department of Laboratory Medicine, Shenzhen Second People's Hospital, the First Affiliated Hospital of Shenzhen University, Shenzhen 518035, China
[c] Department of Bioengineering and COMSET, Clemson University, Clemson, SC, 29634, USA

ARTICLE INFO

*Keywords:*
SPR imaging
Immunosensor
Polymeric microsphere
Hemoglobin
Occult blood tests

ABSTRACT

Occult blood testing is a routine screening method for evaluating the function of the urinary system and digestive tract. The hemoglobin (Hb) content in human excreta is an important indicator of the presence of occult blood. In this study, a surface plasmon resonance imaging (SPRi)-based immunosensor with high sensitivity was developed for the detection of Hb. The immunosensor was constructed by physically immobilizing anti-Hb antibodies on the detection channels. Samples for evaluation were pre-incubated with the polymeric microsphere-antibody conjugate. The shift in resonance wavelength induced by the specific binding of microsphere-antibody-antigen and immobilized antibodies was monitored in real time. Owing to the amplification effect of microspheres, the detection limit of the immunosensor was reduced 42-fold to 4.8 ng/mL under the optimized concentration of immobilized antibody (10 μg/mL) with microsphere-antibody conjugate dilution ratio of 1:200 and incubation time of the microsphere-antibody conjugate and samples (10 min). The immunosensor displayed a good linear response to Hb ranging from 10 ng/mL to 500 ng/mL in both test solutions and in 1:30 urine sample, as well as a good specificity toward Hb and an acceptable recovery rate for spiked Hb solution in urine sample. The immunosensor was also exploited to detect the Hb concentration in 50 clinical urine samples. Therefore, the proposed SPRi immunosensor developed in this study provides a simple, rapid, high-throughput, and sensitive immunology strategy for the detection of occult blood.

## 1. Introduction

The presence of occult blood in human excreta, such as saliva, urine, and feces, is an indicator of chronic and small bleeding from body tissues [1]. Owing to intrinsic advantages such as operational simplicity, low cost, and reliable results, the detection of occult blood in urine and feces has become a routine screening method for evaluating the function of urinary system and digestive tract. Abnormal increase in the hemoglobin (Hb) content of excreta is a manifestation of occult blood and can be related to several diseases, such as inflammation [2,3], stones, and tumors [4]. Chemical assays and immunoassays are two common methods for detecting Hb [5]. Chemical assays were carried out by utilizing the peroxidase activity of the heme portion of the Hb molecule. The dry chemistry method is the most widely used in clinics but is hampered by low sensitivity [6]. In recent years, numerous novel chemical methods with higher sensitivity have been developed by using nanomaterial-based signal enhancement strategies [1,7–9]. However, the specificities of these chemical assays are still not satisfactory because results could be influenced by other substances in the test sample that possess catalytic activity towards hydrogen peroxide. Immunoassays, based on the specific binding of antibodies and antigens, have strong specificity and good sensitivity for Hb detection [10–12]. Colloidal gold immunochromatography strip, the most commonly used immunoassay, is rapid and practical; however, it is qualitative and has low throughput. As such, a high-throughput immunoassay for the quantitative and sensitive measurement of Hb levels is needed.

In recent years, surface plasmon resonance (SPR) detection technology has attracted considerable attention owing to its advantages of simplicity, robustness, label-free, and real-time analysis [13,14]. It has become a central tool for quantitatively studying the dynamics of

* Corresponding authors.
*E-mail addresses:* cjj@szu.edu.cn (J. Chen), shaoyh@szu.edu.cn (Y. Shao).

https://doi.org/10.1016/j.snb.2021.130858
Received 4 July 2021; Received in revised form 25 September 2021; Accepted 29 September 2021
Available online 1 October 2021

biomolecule interactions and is widely used in chemical and biological analyses. SPR imaging (SPRi) sensing technology, a combination of SPR technology with an imaging system, can achieve high-throughput immunosensing, in a 2D array [15,16]. It provides a new strategy for the development of accurate and high-throughput Hb detection and one can readily select the region of interest according to the SPR image of the detection surface. In addition, the sensitivity of the SPR immunosensor is a critical factor that influences the effectiveness of detection. However, due to the lower refractive index perturbation ability induced by biomolecules, the SPR response induced by the direct binding of bare antigen and antibody is relatively small, which may result in a relative higher detection limit that cannot meet the needs of clinical detection for low concentration samples. Therefore, it is necessary to introduce an amplification method to improve the sensitivity of SPR sensing for clinical detection.

A large amount of signal amplification strategies has been developed for biosensors, for instance, enzymatic amplification strategies [17–19] and micro-nano material-based amplification strategies [20–22]. Polymeric microspheres, as emerging functional micro-nano materials, have been used extensively in the fields of biomedicine [23], optics [24], and chemistry [25] owing to their extraordinary physicochemical characteristics such as high specific surface area, low toxicity, ease of functionalization and modification. In the fabrication of biosensors, polymeric microspheres are usually prepared and studied as carriers of molecular recognition elements, which act as probes for target molecules in samples [26–29]. As for SPR-based biosensors, polymeric microspheres were the first-generation nanomaterials used for enhancing SPR sensing [22]. The significant SPR signal enhancement effect is mainly due to the large particle size and molecular weight of polymeric microspheres that lead to a large perturbation in the refractive index of the sensing surface [30,31]. According to the previous reports, the SPR enhancement factors were 30 for human chorionic gonadotropin (hCG) detection [30] and 125 for prostate-specific antigen (PSA) [31] when compared to the experiments without using polymeric microspheres. However, none of these reports have utilized polymeric microspheres-based SPR sensing in the detection of clinical samples.

In this study, unlike the previous reports [30,31] that used polymeric microspheres in the second amplification step, we design a one-step detection strategy that the polymeric microspheres-antibody conjugates are used to capture the target in samples before detection, which improves the simplicity and efficiency of clinical sample detection. Fig. 1 illustrates the detection procedures for immunosensors with or without signal amplification. For the microsphere-amplified strategy, polystyrene (PS) latex microspheres-anti-Hb antibody-2 (PS-anti-Hb-2 for short) conjugates were prepared for Hb adsorption. The SPR response was then induced by the specific interaction of Hb on the microsphere with the anti-Hb antibody-1 (anti-Hb-1 for short) immobilized on the chip, and monitored in real-time. This method was optimized to improve the detection performance of the immunosensor by which process a linear curve was also acquired and the specificity of the immunosensor evaluated. Subsequently, we also verified its detecting performance of Hb in human urine samples. And the amplification effect of the microspheres for SPR sensing is also discussed. Moreover, to the best of our knowledge, the use of SPR immunosensors for occult blood tests has rarely been reported. We believe that our microspheres-based one-step SPRi Hb detection scheme will contribute a lot to the applications in biomedical research studies and clinical detections.

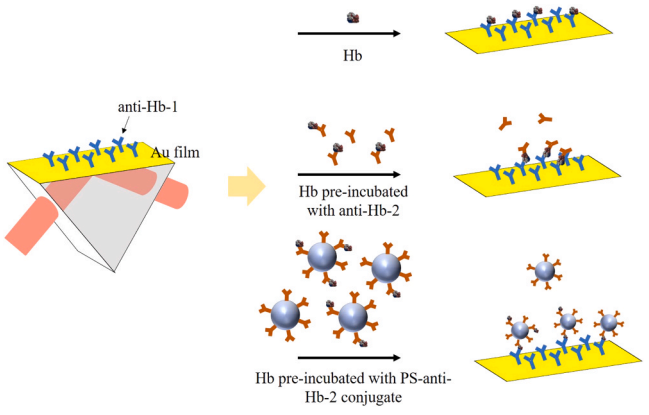


**Fig. 1.** The schematic of detection procedures of immunosensors with or without signal amplification.

## 2. Experimental section

### 2.1. Chemicals

Anti-Hb antibody pair (capture and detector, anti-Hb-1 and anti-Hb-2 for short) are two rabbit monoclonal antibodies to human Hb which can specifically identify different antigenic sites on Hb. Anti-Hb antibody pair and native human Hb was bought from Abcam (Cambridge, Uk). Carboxylate-modified polystyrene (PS) latex microspheres was purchased from Bangs Laboratories' Inc (100 nm in diameter, Indiana, USA). 2-(N-morpholino)-ethanesulfonic acid sodium salt (MES), 1-(3-dimethylaminopropyl)–3-ethylcarbodiimide hydrochloride (EDC), ethanolamine, glucose and bilirubin was bought from Aladdin (Shanghai, China). Bovine serum albumin (BSA), human IgG was obtained from Solarbio Science & Technology Co., Ltd. (Beijing, China). Phosphate buffer saline (PBS, 0.01 mol/L, pH = 7.2), HCl, NaOH was bought from Codow (Guangzhou, China). Human albumin was obtained from Sigma-Aldrich (St. Louis, USA). Human myoglobin (Mb) was purchased from AmyJet Scientific Inc (Wuhan, China). Refractive index matching oil was bought from Cargille-Sacher Laboratories Inc (New Jersey, USA).

### 2.2. Equipment

The wavelength-interrogated SPRi system was developed by this laboratory, and the optical setup and photograph of the system are shown in Fig. 2. Briefly, the white light emitted by a halogen lamp (Daheng Optics, Beijing, China) was first coupled by a liquid-core optical fiber, traveled through a collimator (L1), and then reached the Acousto-Optic Tunable Filter (AOTF, AA Opto-electronic, Orsay, France) to acquire the narrow-band p-polarized light. The light was then expanded by the cylindrical lens group (CL1 and CL2) before reaching the coupling prism. The incident light eventually excited the surface plasma wave (SPW) on the gold surface of the SPR chip, which was coupled to the prism via refractive index matching oil ($n_D = 1.5150$). The SPR chip was fabricated by vacuum evaporation of Cr (2 nm) and Au (48 nm) on BK7 glass (0.5 mm thick). During the experiment, a multichannel homemade PDMS flow cell was mounted on the chip surface. The volume of each channel was 13 μl (1 mm in width, 13 mm in length, and 0.1 mm in height). The reflected light from the prism was finally recorded by the CMOS (Imaging Source, Bremen, Germany) device after traveling through the zoom lens (L2 and L3).

Each time the AOTF altered the wavelength of the incident light, the CMOS was exposed multiple times to obtain an average intensity map of the sensing surface at that specific wavelength. When a full spectrum (640–700 nm) was scanned, the spectral curve (intensity vs wavelength) of each pixel on the sensing surface was obtained. During the study, the AOTF continuously carried out wavelength scanning, and the real-time spectral curves of the regions of interest (ROIs) were acquired by averaging the intensity of all pixels in the ROI at each wavelength within a scanning period. The "generalized polynomial fitting" and "cubic spline interpolation" algorithms were used to fit the spectral curves, to obtain the resonance wavelength (RW) of ROIs, at which the intensity of reflected light was lowest.

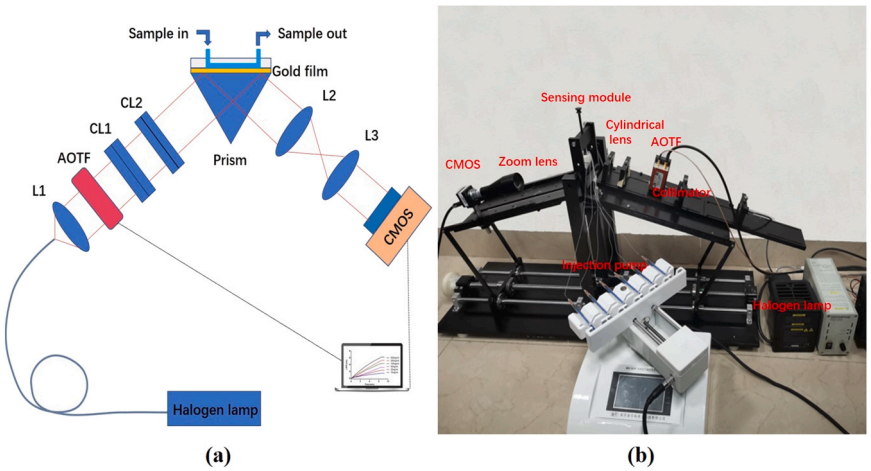


**Fig. 2.** (a) Diagram of the beam path of the SPRi system. (b) Photograph of the SPRi system.

### 2.3. Preparation of PS-anti-Hb-2 conjugate

First, 0.1 mL carboxylic PS microspheres (100 mg/mL) were cleaned twice with MES buffer (0.1 M, pH = 5.3) and then resuspended in 1 mL MES buffer (pH = 5.3). 20 mg of EDC was then added and allowed to incubate for 15 min, with continuous stirring. The mixture was washed twice with PBS buffer (0.01 M, pH = 7.2) and then resuspended in 1 mL PBS. Subsequently, the activated PS microspheres were mixed with 1 mL anti-Hb-2 solution (0.2 mg/mL in PBS) and allowed to incubate for 2 h with constant mixing. The coupling product was washed with the quenching solution (40 mM ethanolamine and 1% BSA in PBS), resuspended in 1 mL quenching solution, and stirred gently for 30 min. Finally, the mixture was washed with storage buffer (0.1% BSA in PBS), resuspended in 1 mL storage buffer, and stored in a refrigerator at 4 °C. The PS-anti-Hb-2 conjugate was diluted before use.

### 2.4. Chip fabrication

The chip was first placed on the prism, and the flow cell was mounted on the chip through spring pressure. PBS was injected to obtain a baseline for each channel. Next, 10 μg/mL of anti-Hb-1 in PBS was then injected for physical adsorption of the antibody onto the Au film. Finally, 10 mg/mL of BSA in PBS was injected to block the residual sites on the chip surface. After each step, PBS solution was injected to wash away the excess substances. The flow rate was set at 10 μl/min for the entire fabrication process.

### 2.5. Detection of Hb in PBS

A standard solution of Hb with a concentration ranging from 10 ng/mL to 500 ng/mL or PBS (control group) was incubated with the PS-anti-Hb-2 conjugate at a dilution ratio of 1:200 and the mixture was stirred continuously for 10 min. The mixture was then injected into the channels at a flow rate of 10 μl/min for 10 min. The RW shift caused by the interaction between the PS-anti-Hb-2-antigen conjugate and the anti-Hb-1 immobilized on the chip was monitored in real time. Then, PBS was injected to wash away the excess substances. To avoid the nonspecific adsorption of PS-anti-Hb-2 conjugate on the chip, the RW shift of control group was subtracted from the RW shift of Hb group to obtain the real-time RW shift (△RW) for Hb group. The value of RW shift ($\triangle RW_{Hb}$) at one minute after the PBS was injected was applied to represent the ultimate SPR response induced by the affinity binding of PS-anti-Hb-2-Hb conjugate with the immobilized anti-Hb-1 at different conditions.

### 2.6. Detection of Hb in urine samples

Fifty morning urine samples were randomly selected from the outpatient population and physical examination population of Shenzhen Second People's Hospital, including 22 males and 28 females. The occult blood tests of urine samples were taken by both dry chemical method and SPR immunosensing method. The dry chemistry examination was carried out using a urine dry chemistry analyzer. For SPR immunosensor, the urine samples were diluted 30 times prior to detection. Then the urine samples were incubated with the PS-anti-Hb-2 conjugate at a dilution ratio of 1:200 and stirred continuously for 10 min. The mixture was then injected into the channels at a flow rate of 10 μl/min for 10 min. The obtained RW shift was brought into the calibration equation to get the concentration of Hb in the samples.

## 3. Results

### 3.1. Optimization

#### 3.1.1. Optimization of the concentration of anti-Hb-1 and dilution ratio of the PS-anti-Hb-2 conjugate

To achieve high sensing performance, for instance, relatively high sensitivity and a broad linear range, we firstly optimized the concentration of anti-Hb-1 immobilized on the chip and the dilution ratio of PS-anti-Hb-2 conjugate that was incubated with Hb. A series of anti-Hb-1 concentrations (5, 10, and 20 μg/mL) were evaluated. In each case, a set of dilution ratios of PS-anti-Hb-2 conjugate (1:400, 1:200, and 1:100) was investigated. Fig. 3a depicts the real-time RW curve of the immobilization process of anti-Hb-1. The 20 μg/mL anti-Hb-1 was rapidly adsorbed onto the chip, and the adsorption amount as well as SPR response reached saturation within 1 min. The 10 μg/mL anti-Hb-1 adsorbed much slower, but the final adsorption amount of 10 μg/mL anti-Hb-1 was comparable to that of the 20 μg/mL anti-Hb-1. The adsorption amount of 5 μg/mL anti-Hb-1 was much less than that of 20 μg/mL and 10 μg/mL anti-Hb-1, and the ultimate RW shift reached only a third of that of 10 μg/mL and 20 μg/mL anti-Hb-1. Fig. 3b-d show the corresponding curve of the RW shift and logarithm of Hb concentration ($lgC_{Hb}$) under different conditions, which confirms the influence of the amount of antibody adsorbed on the binding capacity of Hb. It was observed that for the 10 μg/mL and 20 μg/mL anti-Hb-1 group (Fig. 3b-c), the RW shift was almost equal at the same Hb concentration and dilution ratio of PS-anti-Hb-2 conjugate. The RW shift increased with increasing Hb concentration in the range of 10 ng/mL to 500 ng/mL for 1:200 and 1:400 of PS-anti-Hb-2 conjugate. Moreover, the RW shift of 1:200 PS-anti-Hb-2 conjugate group was greater than that of 1:400 PS-anti-Hb-2 conjugate group at the same Hb concentration. This is

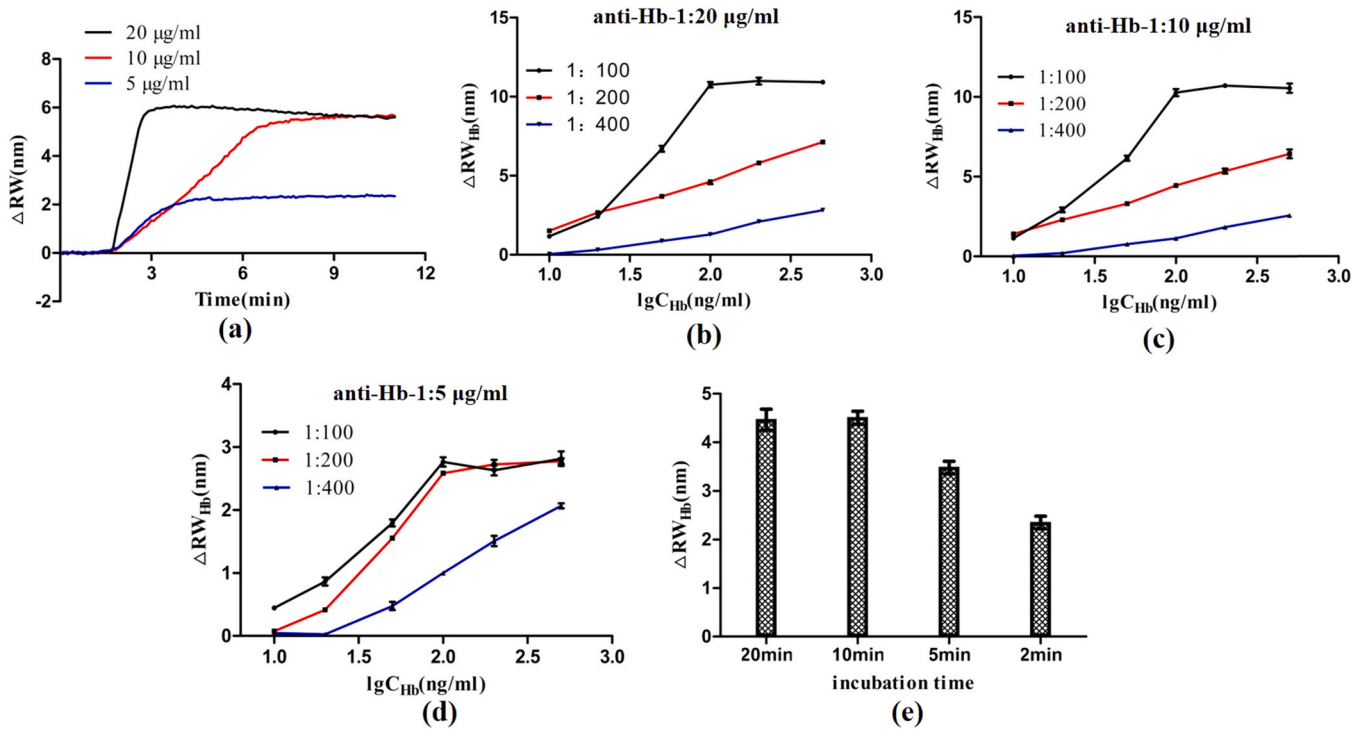


**Fig. 3.** (a) The real-time RW curve of immobilization process of anti-Hb-1. The corresponding curve of the RW shift and logarithm of Hb concentration ($lgC_{Hb}$) at 20 μg/mL anti-Hb-1 (b), 10 μg/mL anti-Hb-1 (c) and 5 μg/mL anti-Hb-1 (d). In each case, the dilution ratio of PS-anti-Hb-2 conjugate was set as 1:400, 1:200, and 1:100. (e) The corresponding relationship between different incubation time (2 min, 5 min, 10 min and 20 min) and the RW shift.

because the binding amount of Hb on the PS-anti-Hb-2 conjugate decreases when the dilution factor increases, thus reducing the binding amount of PS-anti-Hb-2-Hb conjugate on the immobilized antibody, as well as the detection sensitivity. For the 1:100 PS-anti-Hb-2 conjugate, the RW shift increased with increasing Hb concentration in the range of 10 ng/mL-100 ng/mL. When the Hb concentration reached 100 ng/mL, the SPR response reached saturation, which may be due to saturation of the antigen-binding site on the chip surface. In the 5 μg/mL anti-Hb-1

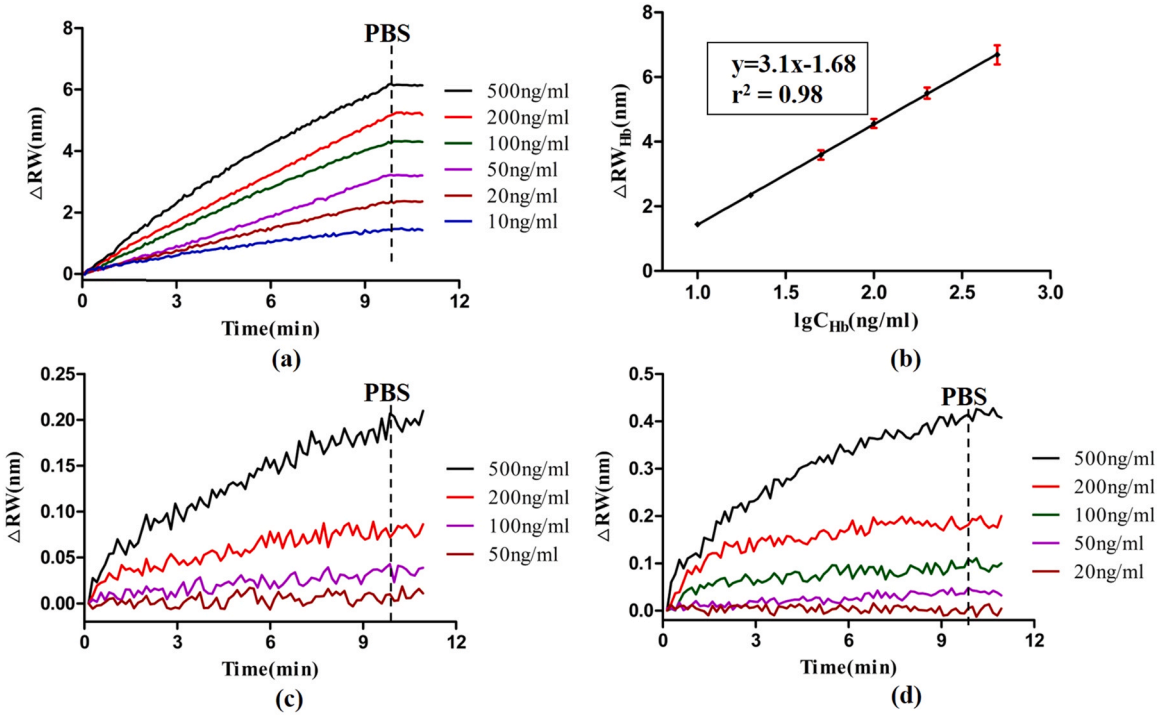


**Fig. 4.** (a) The real-time monitoring of RW shift for the standard solution of Hb pre-incubated with PS-anti-Hb-2 conjugate. (b) The calibration curve of $\triangle RW_{Hb}$ versus $lgC_{Hb}$. (c) The real-time monitoring of RW shift for the standard solution of Hb. (d) The real-time monitoring of RW shift for the standard solution of Hb pre-incubated with anti-Hb-2.

group (Fig. 3d), the RW shift became much smaller than that of the 10 μg/mL and 20 μg/mL antibody groups because of the lack of antigen binding sites on the chip surface. As a result, the detection sensitivity was greatly reduced. For 1:100 and 1:200 of PS-anti-Hb-2 conjugate, when the Hb concentration reached 100 ng/mL, the SPR response reached saturation because of excessive PS-anti-Hb-2-Hb conjugate. In summary, in order to achieve relatively higher detection sensitivity, wider dynamic range, and lower reagent consumption, 10 μg/mL of anti-Hb-1 and 1:200 of PS-anti-Hb-2 conjugate were chosen for the detection of Hb.

#### 3.1.2. Optimization of incubation time of Hb with PS-anti-Hb-2 conjugate

The incubation time of Hb with the PS-anti-Hb-2 conjugate is an important factor for the binding amount of Hb on the PS-anti-Hb-2 conjugate. 1:200 of PS-anti-Hb-2 conjugate was added to 100 ng/mL Hb and stirred continuously for 2 min, 5 min, 10 min, and 20 min. Each sample was then introduced into the detection channels, and the RW shift was monitored. Fig. 3e shows the corresponding relationship between different incubation times and the RW shift. It can be seen that the RW shift increases with increasing incubation time when the incubation time is less than 10 min. There was no noticeable difference in the RW shift between 10 min and 20 min of incubation time. Therefore, 10 min was chosen as the optimum incubation time for Hb detection.

### 3.2. Detection of Hb in solution

Fig. 4a shows the real-time monitoring of RW shift for the standard solution of Hb (10 ng/mL, 20 ng/mL, 50 ng/mL, 100 ng/mL, 200 ng/mL and 500 ng/mL) in PBS pre-incubated with PS-anti-Hb-2 conjugate, which indicates the continuous binding of the PS-anti-Hb-2-antigen conjugate to the anti-Hb-1 immobilized on the chip. It can be seen that the RW shift increases with rising concentration of Hb, and the curves are well separated in less than 5 min. The calibration curve of $\triangle RW_{Hb}$ versus $lgC_{Hb}$ is shown in Fig. 4b, which shows a nearly linear relationship between $\triangle RW_{Hb}$ and $lgC_{Hb}$ in the concentration range of 10 ng/mL to 500 ng/mL. The curve showed the average values of three measurements with error bars showing the standard deviation of three measurements at each data points. The variation coefficient of $\triangle RW_{Hb}$ obtained by different measurement for the same Hb concentration was less than 0.1, which indicated the reproducibility of the proposed sensor. The linear regression equation was $\triangle RW_{Hb} = 3.1 \times lgC_{Hb} - 1.68$ (ng/mL, $r^2 = 0.98$; equation 1). According to the 3σ principle, the detection limit of this method was calculated to be 4.8 ng/mL. To verify the amplification effect of microspheres, the standard solution of Hb, as well as the standard solution of Hb pre-incubated with anti-Hb-2, were injected into the anti-Hb-1 immobilized channels (illustrated in Fig. 1). The real-time RW shift was monitored and plotted in Fig. 4c-d. The data indicated that the $\triangle RW_{Hb}$ of Hb pre-incubated with PS-anti-Hb-2 conjugate group was much larger than that of the Hb group, and Hb pre-incubated with the anti-Hb-2 group. For instance, the $\triangle RW_{Hb}$ of 200 ng/mL Hb pre-incubated with PS-anti-Hb-2 conjugate was 53- and 30- fold higher than that of the 200 ng/mL Hb and 200 ng/mL Hb pre-incubated with anti-Hb-2, respectively. The lowest concentrations that could be detected for Hb and Hb pre-incubated with anti-Hb-2 were approximately 200 ng/mL and 100 ng/mL, respectively, which were 42- and 21-fold higher than that of Hb pre-incubated with PS-anti-Hb-2 conjugate. It could be concluded that the sensitivity of the immunosensor was greatly improved owing to the signal amplification effect of the microspheres.

The properties of the developed SPR immunosensor were compared with those of other sensors for urine occult blood tests based on different sensing methods. Table S1 summarizes the methods, fabrication, dynamic detection range, detection limits, and detection time of these sensors. The detection limit of the developed sensor was superior to that of the other methods. For occult blood tests, high sensitivity would allow a high dilution ratio of the samples during the test, which could reduce the effect of interference on the test. Moreover, the time required for Hb detection was shorter than that required for the other methods. Additionally, this immunosensor was easy to fabricate and could detect multiple samples simultaneously.

### 3.3. Detection of Hb in urine samples

Fig. 5a depicted the real-time monitoring of RW shift for the standard solution of Hb in 1:30 urine sample and the inset showed the linear calibration plot corresponding to the increase of $\triangle RW_{Hb}$ with the increasing $lgC_{Hb}$. The urine sample was collected from a healthy woman who has been tested negative for urine occult blood. According to previous reports, the Hb concentration in the urine of healthy people is generally below 300 ng/mL, which is also the detection limit of dry chemistry method for Hb in clinic. Since the lower limit of detection range was 10 ng/mL, the urine sample could be diluted 30 times prior to detection. As shown in Fig. S1, the diluted urine sample did not induce obvious SPR response, which indicated that the Hb concentration in the diluted urine sample was below the detection limit of the sensor. The Hb standard solution in urine sample was prepared at concentrations ranging from 300 ng/mL to 15 μg/mL and diluted 30 times prior to detection. As seen in Fig. 5a, the linear regression equation was calculated as $\triangle RW_{Hb} = 3.24 \times lgC_{Hb} - 1.93$ (ng/mL, $r^2 = 0.98$, equation 2), which was similar with equation 1, indicating that the actual urine sample has an invisible effect on detection. The recovery analysis was conducted by detecting the SPR response of 450 ng/mL, 1400 ng/mL and 7000 ng/mL Hb in urine sample. The samples were diluted 30 times prior to detection. The obtained RW shift was brought into equation 1 to get the actual detected concentration. The recovery rate (% recovery) was calculated and shown in Table S2. The recoveries of 450 ng/mL, 1400 ng/mL and 7000 ng/mL Hb were 94.2%, 108.3% and 106.5% respectively, which were all between 90% ~ 110% range. The selectivity of the developed sensor was explored by detecting the response of four kinds of interfering substances: albumin, Mb, bilirubin, and glucose that possibly co-exist in the urine samples. The albumin, Mb, bilirubin, and glucose were prepared in the artificial urine at concentrations of 150 μg/mL, 4 μg/mL, 6 μg/mL, and 600 μg/mL, respectively, which are the positive critical values of these substances in urine samples. The samples were diluted 30 times prior to detection. As shown in Fig. 5b, when compared to 10 ng/mL Hb in 1:30 artificial urine, albumin, Mb, bilirubin and glucose did not induce a noticeable SPR response, indicating that the sensor has a good specificity toward Hb.

The potential of the proposed sensor being used as a clinical diagnostic tool was explored by detecting the Hb concentration in urine samples. And the Hb concentration results obtained from the proposed sensor were compared with the results of dry chemistry occult blood test. For dry chemical occult blood test, the corresponding range of Hb concentration of negative, ± , 1 + , 2 + and 3 + samples was < 300 ng/mL, 300–600 ng/mL, 600–2000 ng/mL, 2000–10,000 ng/mL and > 10,000 ng/mL, respectively. According to the Hb concentration in the urine samples measured by SPR immunosensing method, the samples were grouped according to the above five concentration ranges. Tables 1 and S3 are the comparisons of occult blood detection results of 50 clinical urine samples by SPR immunosensing method and dry chemical method. It can be seen that the negative rate of occult blood detected by SPR immunosensing method is 54% (27/50), and the negative rate of occult blood detected by dry chemical method is 58% (29/50). Among the samples which were identified as strong occult blood positive (2+, 3+) by dry chemical method, the probability that the Hb concentration detected by SPR immunosensing method was higher than 300 ng/mL was 88.9% (8/9), which indicates the high consistency of two detection methods in this concentration range. However, among the samples which were identified as weak occult blood positive (±, 1+) by dry chemical method, the probability that the Hb concentration detected by SPR immunosensing method was higher than 300 ng/mL was 50% (6/12). And among the samples which were identified as occult blood

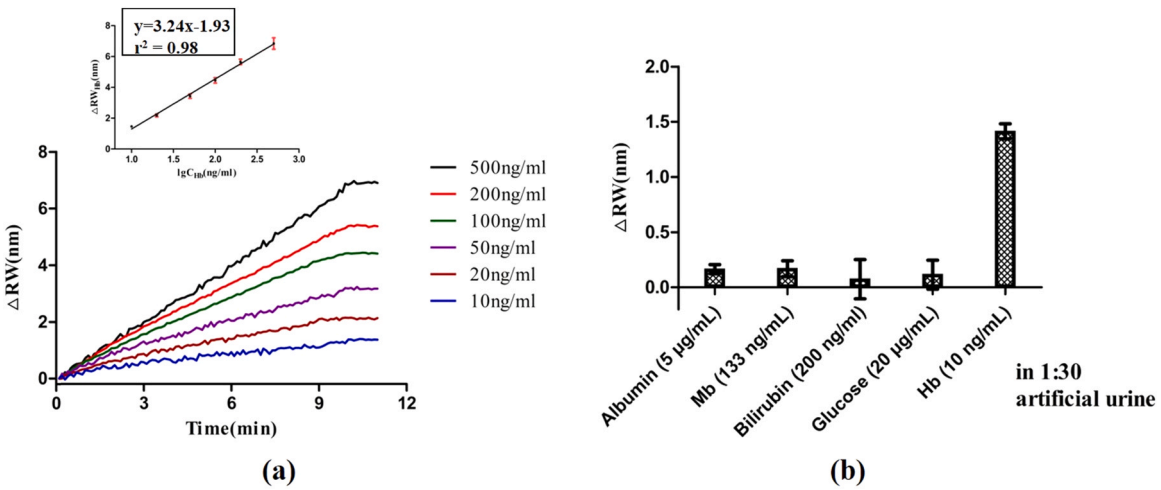


**Fig. 5.** (a) The real-time monitoring of RW shift for the standard solution of Hb in 1:30 urine sample pre-incubated with PS-anti-Hb-2 conjugate. The inset is the calibration curve of $\triangle RW_{Hb}$ versus $lgC_{Hb}$. (b) The $\triangle RW_{Hb}$ corresponds to 5 μg/mL albumin, 133 ng/mL Mb, 200 ng/mL bilirubin, 20 μg/mL glucose and 10 ng/mL Hb in 1:30 artificial urine.

**Table 1**
The comparison of occult blood detection results of 50 clinical urine samples by SPR immunosensing method and dry chemical method.

| Dry chemistry method | SPR immunosensing method (ng/mL) | | | | | |
|---|---|---|---|---|---|---|
| | <300 | 300–600 | 600–2000 | 2000–10,000 | >10,000 | Total amount |
| negative | 20 | 5 | 3 | 1 | | 29 |
| ± | 1 | 1 | | | | 2 |
| 1+ | 5 | 2 | 2 | 1 | | 10 |
| 2+ | 1 | 2 | | 1 | | 4 |
| 3+ | | 1 | 2 | 1 | 1 | 5 |
| Total amount | 27 | 11 | 7 | 4 | 1 | 50 |

negative by dry chemical method, the probability that the Hb concentration detected by SPR immunosensing method was lower than 300 ng/mL was 69% (20/29). The inconsistency of results for weak positive and negative samples might be caused by the following reasons: 1. The dry chemical method can not only detect the free Hb in urine samples, but also detect the Hb in red blood cells, while SPR immunosensing method can only detect free Hb in urine samples. Therefore, the Hb concentration detected by dry chemical method might be higher than that of SPR immunosensing method. 2. The results of dry chemical method could be influenced by other substances in the test sample that possess catalytic activity towards hydrogen peroxide, such as Mb, peroxidase produced by bacteria and unstable enzyme, which may cause false positive results. 3. The coexistence of reduced glutathione, vitamin C and other reducing agents could competitively inhibit the reaction, which may cause false negative results. Although the SPR immunosensing method cannot detect the Hb inside red blood cells, it possesses strong specificity towards Hb. As a result, the probability of false positive and false negative for free Hb detection is relatively small. Thus, it can be exploited to detect hemoglobinuria and has great potential in the detection of hemolytic diseases.

## 4. Discussion

In this study, a SPRi immunosensor was developed to detect Hb levels. The sensitivity of immunosensor is greatly enhanced by the adoption of microspheres, the amplification effect of which is predominantly due to the increased surface mass load. However, many other factors related to microspheres may also affect the signal amplification. As illustrated in Fig. 6, the binding process of the PS-anti-Hb-2-antigen conjugate on the immobilized anti-Hb-1 can be described in two steps [32,33]. First, the analyte diffuses out of the bulk forced convective flow

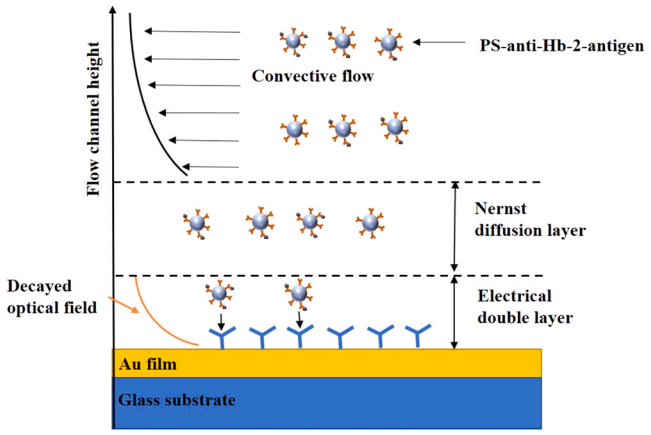


**Fig. 6.** The illustration of the binding process of PS-anti-Hb-2-antigen conjugate on the immobilized anti-Hb-1.

region and passes through the Nernst diffusion layer near the surface of the sensor. The stagnant Nernst diffusion layer has a dimension of several micrometers, where particle diffusion is dominated with a rather low convective flow. Second, the actual antibody–antigen interaction occurs in the electrical double-layer region, which has a thickness of several nanometers [32,33]. The width and height of the rectangular microfluidic channel were 1000 μm and 100 μm, respectively. The flow rate was set to 10 μl/min. Therefore, the lateral velocity of flow was calculated to be 1670 μm/s with a Reynolds number of approximately 0.16, which is beneficial for biomolecule interactions [34]. Therefore, the low Reynolds number nature of a fluid can be applied. Typically, the hydrodynamic diameter of an antigen molecule is less than 10 nm. Its

conjugation with PS-anti-Hb-2 (≈150 nm in diameter) greatly increases the antigen entrance possibilities across the diffusion layer to the sensing surface because of the shear gradient lift force [35]. More importantly, when a PS-anti-Hb-2-antigen conjugate is closer to the gold surface, it can enlarge the variation of the refractive index when binding on the surface. However, compared to a bare antigen itself, the PS can experience a larger optical gradient attraction force induced by the decayed optical field of the surface plasmon polariton [36,37]. Particle–surface interaction forces such as van der Waals force and electrical attraction force can also hold the PS-anti-Hb-2-antigen conjugate for tight binding with the anti-Hb-1 on the gold surface [38,39].

It should be noted that a larger size of the PS will provide a stronger binding signal enhancement, however a larger particle size will increase the convective drag force due to Stokes' law. In addition, the wall-effect lift force that pushes the PS away from the gold surface will significantly increase with a larger particle size owing to fourth-order dependence [40]. These two hydrodynamic forces can break the antibody-antigen binding force on the gold surface. Therefore, in this study a PS size of 100 nm was chosen, which is in the near-field region of the optical attraction force while minimizing the influence of unwanted hydrodynamic forces. For the bare PS-antibody conjugate, the possibility of contact with the surface is greatly reduced because of the lack of affinity interaction and as such, no SPR signal was observed. Moreover, it was postulated that the PS size could be further optimized for different biomolecule counterparts.

In this study, the direct physical adsorption of Hb antibody onto the gold surface of the SPR chip was used for antibody immobilization due to its simplicity. However, it may lead to the loss of antibody activity due to the poor orientation, steric hindrance and conformational changes occurring along the immobilization process. The influence of physical adsorption on the assay sensitivity should be studied. We have compared the performance of two immobilization methods for Hb detection: physical adsorption and covalent bonding (Supporting Information). It was found that the physical adsorption performed better than covalent bonding in the sensitivity for detecting Hb (Fig. S2). Moreover, covalent bonding is time-consuming and tedious. Thus the physical adsorption was chosen as the immobilization method for antibodies.

The reutilization of the proposed sensor has also been explored. Firstly, 50 ng/mL of Hb pre-incubated with PS-anti-Hb-2 conjugate was injected into the channels and bound on the anti-Hb-1. The dissociation of Hb from anti-Hb-1 was performed using 50 mM NaOH in pure water, followed by PBS. The binding and dissociation were repeated for several times. As seen in Fig. S3, the binding capacity of antibody didn't get worse at the first one reutilization process. After the second reutilization process, the $\triangle RW_{Hb}$ decreased to 82% of the initial level. And the $\triangle RW_{Hb}$ further decreased to 71% of the initial level after the third reutilization process. The reutilization of the proposed sensor is not satisfying when compared with commercial SPR chips, which may be derived from the low stability of antibodies on the chip surface. It is possible that the reutilization of the proposed sensor could be improved by other regeneration methods or reagents.

## 5. Conclusion

In this paper, a novel, sensitive, and high-throughput SPR immunosensor for rapid detection of Hb was developed. A wavelength-interrogated SPR imaging system was built based on swept-source technology. Owing to the amplification effect of microspheres, the immunosensor had the capacity to determine Hb from 10 ng/mL to 500 ng/mL under optimized condition. The detection limit of immunosensor was reduced to as low as 4.8 ng/mL, which is 42 times smaller than that of the traditional SPR immunosensing scheme. The immunosensor also displayed a good specificity toward Hb and an acceptable recovery rate for spiked Hb solution in urine sample. Finally, the immunosensor was successfully used for the determination of Hb in urine samples. In summary, this SPR immunosensor provides an efficient alternative immunological strategy for occult blood tests.

## CRediT authorship Contribution statement

Author Contributions: conceptualization, J. Zhou, J. Chen and Y. Shao; Methodology, J. Zhou; Validation, J. Zhou, X. Wang and Y. Zeng; Investigation, J. Zhou, X. Wang and Y. Zeng; Resources, D. Gu and Y. Shao; Writing – original draft preparation, J. Zhou; Writing – review and editing, Bruce Zhi Gao, J. Chen and Y. Shao; Visualization, J. Zhou; Supervision, Y. Shao; Funding acquisition, J. Chen and Y. Shao.

## Declaration of Competing Interest

The authors declare that they have no known competing financial interests or personal relationships that could have appeared to influence the work reported in this paper.

## Acknowledgements

This work was supported by the Project from National Natural Science Foundation of China (61775148, 61527827, and 61905145); National Key Research and Development Program of China (2017 YFB0403804); Guangdong Natural Science Foundation and Province Project (2017B020210006, 2018A030310544, 2021A1515011916); Shenzhen Science and Technology R&D and Innovation Foundation (JCYJ20200109105608771, JCYJ20180305124754860, JCYJ201802 28162956597).

### *Disclosures*

The authors declare no conflicts of interest.

## Appendix A. Supporting information

Supplementary data associated with this article can be found in the online version at doi:10.1016/j.snb.2021.130858.

## References

[1] Y. Jiang, Z. Sun, L. Zhang, Y. Qiao, F. Liu, Y. Cai, W. Zhang, Q. Zhang, Z. Duan, H. Wang, Encapsulating chromogenic reaction substrates with porous hydrogel scaffolds onto arrayed capillary tubes toward a visual and high-throughput colorimetric strategy for rapid occult blood tests, J. Mater. Chem. B 5 (2017) 1159–1165.
[2] C.J. Gill, J. Lau, S.L. Gorbach, D.H. Hamer, Diagnostic accuracy of stool assays for inflammatory bacterial gastroenteritis in developed and resource-poor countries, Clin. Infect. Dis. 37 (2003) 365–375.
[3] N. Ishida, T. Miyazu, R. Takano, S. Tamura, S. Tani, T. Kagami, M. Yamade, Y. Hamaya, M. Iwaizumi, S. Osawa, T. Furuta, H. Miyajima, K. Sugimoto, Prostaglandin E-major urinary metabolite versus fecal immunochemical occult blood test as a biomarker for patient with ulcerative colitis, BMC Gastroenterol. 20 (2020) 114.
[4] J.D. Hardcastle, J.O. Chamberlain, M.H. Robinson, S.M. Moss, S.S. Amar, T. W. Balfour, P.D. James, C.M. Mangham, Randomised controlled trial of faecal-occult-blood screening for colorectal cancer, Lancet 348 (1996) 1472–1477.
[5] B. Koscielniak-Merak, B. Radosavljevic, A. Zajac, P.J. Tomasik, Faecal occult blood point-of-care tests, J. Gastrointest. Cancer 49 (2018) 402–405.
[6] X. Xu, C. Luo, J. Pu, Q. Liu, Y. Zhang, Reliability of dry-chemistry method in detecting urine occult blood, Chongqing Med. 41 (2012) 1802–1804.
[7] Y. Wu, Y. Chen, Y. Li, J. Huang, H. Yu, Z. Wang, Accelerating peroxidase-like activity of gold nanozymes using purine derivatives and its application for monitoring of occult blood in urine, Sens. Actuators B-Chem. 270 (2018) 443–451.
[8] J. Pollard, O. Rifaie-Graham, S. Raccio, A. Davey, N.J.A.C. Bruns, Biocatalytically initiated precipitation ATRP as a quantitative method for hemoglobin detection in biological fluids, Anal. Chem. 92 (2019) 1162–1170.
[9] N. Swaminathan, Y. Nerthigan, H.-F. Wu, Polyaniline stabilized silver (I) oxide nanocubes for sensitive and selective detection of hemoglobin in urine for hematuria evaluation, Microchem. J. 155 (2020), 104723.
[10] P. Wang, H. Liu, T. Zhang, Y. Cao, Effect of in vitro gastrointestinal environment on immunochemical fecal occult blood test, Chin. J. Lab. Med. 40 (2017) 294–297.
[11] Y. Li, Z. Dai, F. Liao, Evaluation and analysis of three methods of occult blood test, J. Chongqing Med. Univ. 43 (2018) 1212–1216.

[12] S.H. Elsafi, N.I. Alqahtani, N.Y. Zakary, E.M. Al Zahrani, The sensitivity, specificity, predictive values, and likelihood ratios of fecal occult blood test for the detection of colorectal cancer in hospital settings, Clin. Exp. Gastroenterol. 8 (2015) 279–284.
[13] J. Zhou, Y. Zeng, X. Wang, C. Wu, Z. Cai, B.Z. Gao, D. Gu, Y. Shao, The capture of antibodies by antibody-binding proteins for ABO blood typing using SPR imaging-based sensing technology, Sens. Actuators B: Chem. 304 (2020), 127391.
[14] Y. Zeng, J. Zhou, X. Wang, Z. Cai, Y. Shao, Wavelength-scanning surface plasmon resonance microscopy: A novel tool for real time sensing of cell-substrate interactions, Biosens. Bioelectron. 145 (2019), 111717.
[15] C.L. Wong, M. Olivo, Surface plasmon resonance imaging sensors: a review, Plasmonics 9 (2014) 809–824.
[16] Y. Zeng, R. Hu, L. Wang, D. Gu, J. He, S.Y. Wu, H.P. Ho, X. Li, J. Qu, B.Z. Gao, Y. Shao, Recent advances in surface plasmon resonance imaging: detection speed, sensitivity, and portability, Nanophotonics 6 (2017) 1017–1030.
[17] H. Xia, J. Huang, X. Lu, G. Wang, Z. Zhang, J. Yue, Q. Li, S. Wang, J. Yan, L. Deng, Y. Xiang, Autocatalytic MNAzyme-integrated surface plasmon resonance biosensor for simultaneous detection of bacteria from nosocomial bloodstream infection specimens, Sens. Actuators B: Chem. 330 (2021), 129255.
[18] E. Salinas, V. Rivero, A. Torriero, D. Benuzzi, M.I. Sanz, J. Raba, Multienzymatic-rotating biosensor for total cholesterol determination in a FIA system, Talanta 70 (2006) 244–250.
[19] L. He, R. Huang, P. Xiao, Y. Liu, L. Jin, H. Liu, S. Li, Y. Deng, Z. Chen, Z. Li, N. He, Current signal amplification strategies in aptamer-based electrochemical biosensor: a review, Chin. Chem. Lett. 32 (2021) 1593–1602.
[20] L. Syedmoradi, A. Ahmadi, M.L. Norton, K. Omidfar, A review on nanomaterial-based field effect transistor technology for biomarker detection, Mikrochim. Acta 186 (2019) 739.
[21] S.H. Lee, J.H. Sung, T.H. Park, Nanomaterial-based biosensor as an emerging tool for biomedical applications, Ann. Biomed. Eng. 40 (2012) 1384–1397.
[22] S. Zeng, D. Baillargeat, H.-P. Ho, K.-T. Yong, Nanomaterials enhanced surface plasmon resonance for biological and chemical sensing applications, Chem. Soc. Rev. 43 (2014) 3426–3452.
[23] K. Saralidze, L.H. Koole, M.L.W. Knetsch, Polymeric microspheres for medical applications, Materials 3 (2010) 3537–3564.
[24] J. Ward, O. Benson, WGM microresonators: sensing, lasing and fundamental optics with microspheres, Laser Photonics Rev. 5 (2011) 553–570.
[25] J. Zhang, J. Chen, Q. Zhang, R. Wang, S. Wu, Polymeric microsphere-loaded palladium-iminodiacetic acid complex as an efficient and easily recycled catalyst for Suzuki reaction in ionic liquid, Res. Chem. Intermed. 45 (2019) 2503–2514.
[26] R. Hara, H. Kawaguchi, Highly sensitive detection of telomerase by using G-Quartet DNA binder conjugated polymeric microspheres, Kobunshi Ronbunshu 69 (2012) 122–128.
[27] N. Ma, C. Ma, N. Wang, C. Li, S. Elingarami, X. Mou, Y. Tang, S. Zheng, N. He, Application of functional microsphere in human hepatitis B virus surface antigen detection, J. Nanosci. Nanotechnol. 14 (2014) 3348–3355.
[28] T.M. Blicharz, W.L. Siqueira, E.J. Helmerhorst, F.G. Oppenheim, P.J. Wexler, F. F. Little, D.R. Walt, Fiber-optic microsphere-based antibody array for the analysis of inflammatory Cytokines in saliva, Anal. Chem. 81 (2009) 2106–2114.
[29] J. Wang, L. Ren, X. Wang, Q. Wang, Z. Wan, L. Li, W. Liu, X. Wang, M. Li, D. Tong, A. Liu, B. Shang, Superparamagnetic microsphere-assisted fluoroimmunoassay for rapid assessment of acute myocardial infarction, Biosens. Bioelectron. 24 (2009) 3097–3102.
[30] A.H. Severs, R.B.M. Schasfoort, Enhanced surface plasmon resonance inhibition test (ESPRIT) using latex particles, Biosens. Bioelectron. 8 (1993) 365–370.
[31] G. Besselink, A. Kooyman, bP.J.H.Jv Os, G. Engbers, R. Schasfoorta, Signal amplification on planar and gel-type sensor surfaces in surface plasmon resonance-based detection of prostate-specific antigen, Anal. Biochem. 333 (2004) 165–173.
[32] C. Low, R. Wills, F. Walsh, Electrodeposition of composite coatings containing nanoparticles in a metal deposit, Surf. Coat. Technol. 201 (2006) 371–383.
[33] R.B. Schasfoort, Handbook of surface plasmon resonance, Royal Society of Chemistry,, 2017.
[34] G. Hu, Y. Gao, D. Li, Modeling micropatterned antigen–antibody binding kinetics in a microfluidic chip, Biosens. Bioelectron. 22 (2007) 1403–1409.
[35] J.M. Martel, M. Toner, Inertial focusing in microfluidics, Annu. Rev. Biomed. Eng. 16 (2014) 371–396.
[36] V. Garcés-Chávez, R. Quidant, P. Reece, G. Badenes, L. Torner, K. Dholakia, Extended organization of colloidal microparticles by surface plasmon polariton excitation, Phys. Rev. B 73 (2006), 085417.
[37] Z. Fang, F. Lin, S. Huang, W. Song, X. Zhu, Focusing surface plasmon polariton trapping of colloidal particles, Appl. Phys. Lett. 94 (2009), 063306.
[38] M.M. Hatlo, L. Lue, The role of image charges in the interactions between colloidal particles, Soft Matter 4 (2008) 1582–1596.
[39] P. Schein, P. Kang, D. O'Dell, D. Erickson, Nanophotonic force microscopy: characterizing particle–surface interactions using near-field photonics, Nano Lett. 15 (2015) 1414–1420.
[40] D. Di Carlo, Inertial microfluidics, Lab a Chip 9 (2009) 3038–3046.

**Jie Zhou** obtained her Ph.D. degree in Biomedical Engineering from Zhejiang University, China. Currently, she is an associate researcher at Key Laboratory of Optoelectronic Devices and Systems of Ministry of Education and Guangdong Province, Shenzhen University. Her research interests involve the application of SPR biosensors, electrochemical biosensors and nanosensors in biomedical area.

**Xueliang Wang** obtained his master degree in Optics from Shenzhen University, China. Currently, he is a research associate at Key Laboratory of Optoelectronic Devices and Systems of Ministry of Education and Guangdong Province, Shenzhen University. His research interests include the development of SPR system.

**Jiajie Chen** obtained his Ph.D. in Electronic Engineering from the Chinese University of Hong Kong (CUHK) in 2016. After working as a postdoctoral fellow in the CUHK and University of California San Diego. In 2019, he joined the Key Laboratory of Optoelectronic Devices and Systems of Ministry of Education and Guangdong Province in Shenzhen University as an Assistant Professor. His research interests include optofluidics, surface plasmon resonance biosensors, and optical tweezers.

**Youjun Zeng** obtained his Ph.D. degree in Optics from Shenzhen University, China. Currently, he is a post-doctor at Key Laboratory of Optoelectronic Devices and Systems of Ministry of Education and Guangdong Province, Shenzhen University. His research interests include the development and applications of SPR system.

**Dayong Gu** earned his M.D. degree from Third Military Medical University. Currently, he is a senior researcher at Health Science Center in Shenzhen Second People's Hospital, the First Affiliated Hospital of Shenzhen University. His research interests include microbial molecular diagnostic techniques, optical biosensors and surface plasmon resonance sensors.

**Bruce Zhi Gao** obtained his Ph.D. degree in Biomedical Engineering from University of Miami, USA. Currently, he is a professor at Department of Bioengineering, Clemson University. His research interests involve optical Imaging, microfabrication and cell-ECM Interaction.

**Yonghong Shao** obtained his Ph.D. degree in Optics from Changchun Institute of Optics, Fine Mechanics and Physics, Chinese Academy of Science, China. Currently, he is a professor at Key Laboratory of Optoelectronic Devices and Systems of Ministry of Education and Guangdong Province, Shenzhen University. His research interests involve surface plasmon resonance sensors, fluorescence imaging and confocal endoscopy. He has published over 40 papers and 17 Chinese patents.